



ELSEVIER

Journal of Chromatography A, 857 (1999) 1–20

JOURNAL OF
CHROMATOGRAPHY A

www.elsevier.com/locate/chroma

Reversed-phase liquid chromatographic separation of complex samples by optimizing temperature and gradient time

I. Peak capacity limitations

J.W. Dolan^a, L.R. Snyder^{a,*}, N.M. Djordjevic^b, D.W. Hill^c, T.J. Waeghe^d

^aLC Resources Inc., 2930 Camino Diablo, Suite 110, Walnut Creek, CA 94596, USA

^bNovartis Pharma AG, Basel 4002, Switzerland

^cMicrochemistry Laboratory, University of Connecticut, Storrs, CT 91107, USA

^dDu Pont Co., Experimental Station, P.O. Box 8040, Wilmington, DE 19980, USA

Received 27 November 1998; received in revised form 27 May 1999; accepted 25 June 1999

Abstract

The separation of samples that contain more than 15 to 20 analytes ($n > 15-20$) is typically difficult and usually requires gradient elution. We have examined the reversed-phase liquid chromatographic separation of 24 samples with $8 \leq n \leq 48$ as a function of temperature T and gradient time t_G . The required peak capacity was determined for each sample, after selecting T and t_G for optimum selectivity and maximum sample resolution. Comparison of these results with estimates of the maximum possible peak capacity in reversed-phase gradient elution was used to quantify the maximum value of n for some required sample resolution (when T and t_G have been optimized). These results were also compared with literature studies of similar *isocratic* separations as a function of ternary-solvent mobile phase composition, where the proportions of methanol (MeOH), tetrahydrofuran (THF) and water were varied simultaneously. This in turn provides information on the relative effectiveness of these two different method development procedures (optimization of T and t_G vs. % MeOH and % THF) for changing selectivity and achieving maximum resolution. © 1999 Elsevier Science B.V. All rights reserved.

Keywords: Optimization; Peak capacity; Temperature effects; Gradient elution; Computer simulation; Mobile phase composition; Resolution; Selectivity

1. Introduction

The usual goal of high-performance liquid chromatography (HPLC) method development is an adequate separation of all sample compounds of interest within an acceptable run time. In most cases, it is possible to achieve this objective by a systematic variation of separation conditions [1]. As the number n of sample components increases, however, it

becomes increasingly difficult to separate all compounds of interest in a single chromatographic run. This difficulty can be overcome to some extent by carrying out multi-variable optimization for improved selectivity and band spacing; some previous examples are summarized in Table 1. However, this approach can lead to a rapid increase in the required number of method development experiments. Ultimately, for samples which contain a sufficiently large number of components and whose bands are crowded together in resulting chromatograms, it

*Corresponding author.

Table 1

Some examples of HPLC method development which involve the simultaneous variation of two experimental conditions

1. Quaternary-solvent mobile phase [MeOH, THF, acetonitrile (ACN) and water] with solvent-strength (and run time) held constant [3]
2. Ternary-solvent mobile phase (MeOH, ACN, water or MeOH, THF, water), with solvent-strength allowed to vary [4]
3. Binary-solvent mobile phase with pH and ion-pairing-reagent concentration varied [5]
4. Column type and mobile phase % organic allowed to vary [6]
5. Mobile phase pH and % organic allowed to vary [7]
6. Temperature and gradient steepness allowed to vary [8]

becomes impractical to attempt their separation by any single chromatographic method. We will refer to this situation, illustrated by the example of Fig. 1, as one of *limited peak capacity*. Here, there is simply not enough room (capacity) in the chromatogram to allow all peaks to be resolved from each other. The sample of Fig. 1 contains 48 different components; an arbitrary choice of separation temperature ($T=50^{\circ}\text{C}$) and gradient time ($t_G=40$ min) results in two overlapping triplets (“3” in Fig. 1) plus six overlapping doublets (“2” in Fig. 1). This behavior is typical for a random distribution of a large number of peaks within a finite chromatogram [2].

The present paper examines the peak capacity required for different values of n , when temperature (T) and gradient steepness (t_G) are optimized. By

comparing these required peak capacities with values that are readily obtainable, it is possible to set a rough limit on the maximum value of n , such that an acceptable separation of all components is likely in a single run. One alternative to conventional method development for large- n samples is explored in the following paper [9], namely the combined use of two or more separations in place of a single HPLC run.

2. Theory

2.1. Peak capacity definitions

The hypothetical example of Fig. 2 will be used to illustrate the various definitions of peak capacity

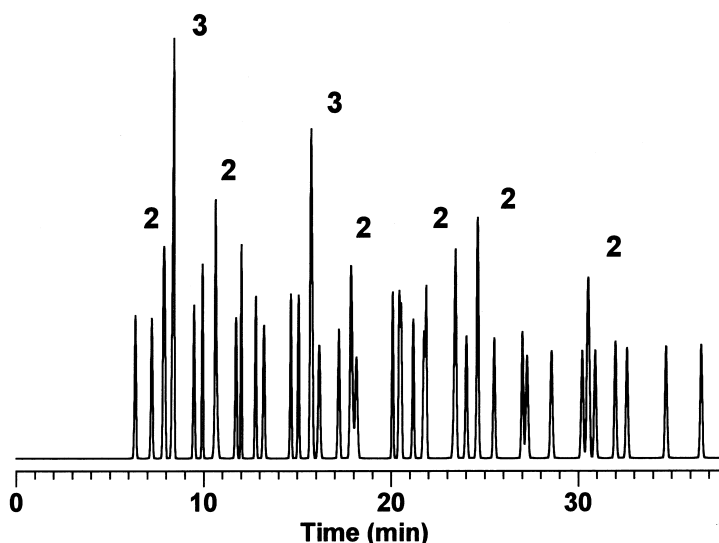


Fig. 1. Separation of a 48-component sample. Computer simulation based on experimental data. Other conditions are: 0–100% acetonitrile in buffer gradient in 40 min, temperature 50°C , 25×0.46 cm column, 2.0 ml/min. Sample is a mixture of basic, acidic and neutral drugs plus nitroalkane internal standards as described in Ref. [9], except that basic drugs 1–7 plus nitromethane and nitroethane were omitted because they elute before the arrival of the gradient at the column inlet. Numbers in figure refer to unresolved ($R_s < 0.5$) doublets (“2”) or triplets (“3”); since the various bands are of equal area, doublets and triplets are taller than singlets.

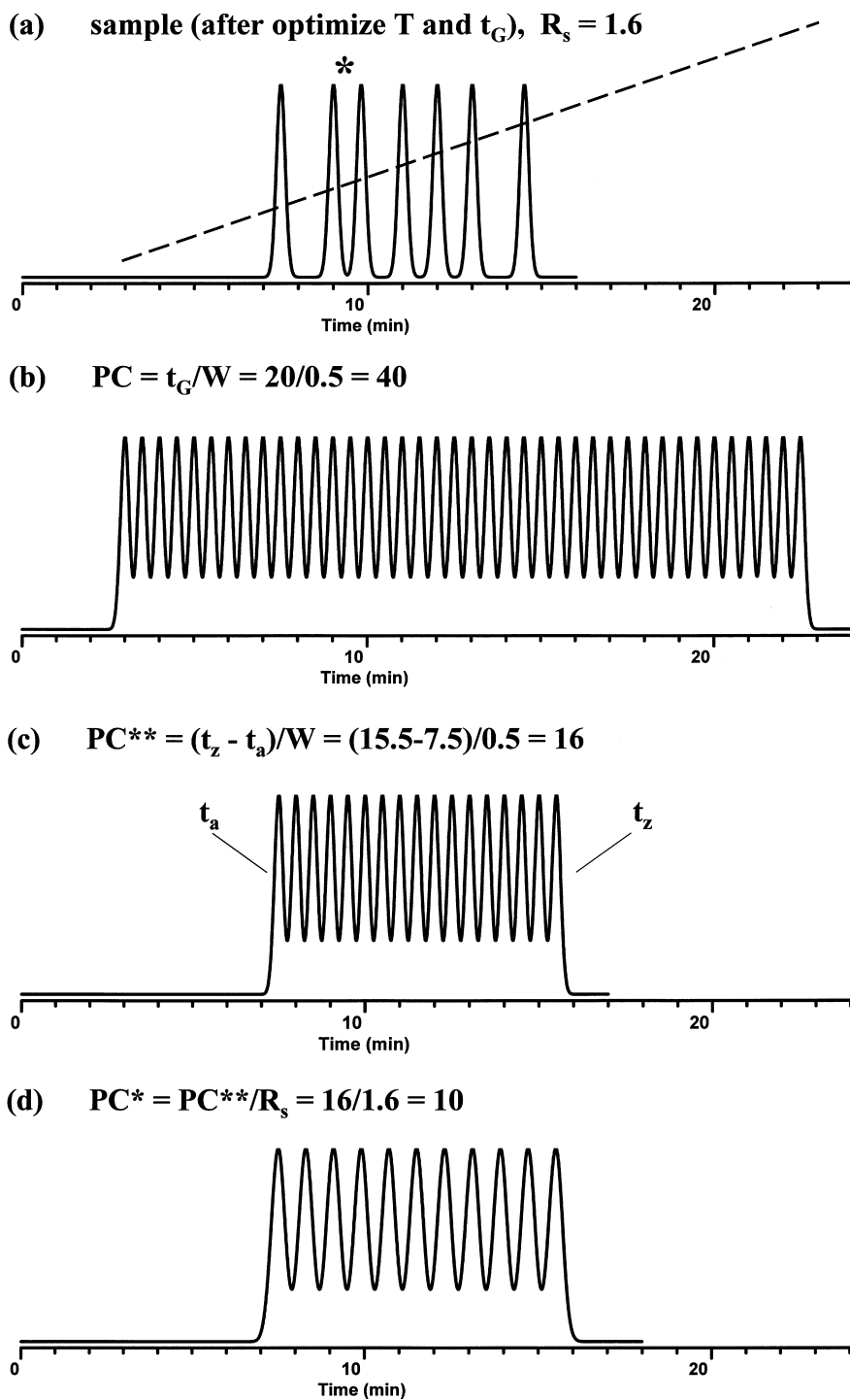


Fig. 2. Peak capacity after optimizing temperature and gradient time (hypothetical separations). (a) Observed separation for maximum resolution R_s ; (b) illustration of peak capacity PC for separation of (a); (c) illustration of sample peak capacity PC^{**} for separation of (a); (d) illustration of required sample peak capacity PC^* for separation of (a).

used in the present study. Fig. 2a shows the separation of a hypothetical sample, after T and t_G have been optimized for maximum sample resolution; the “critical” (least resolved) pair of bands is indicated by an (*), for which $R_s = 1.6$. A 0–100% B gradient in 20 min is assumed in Fig. 2a. The dashed line in Fig. 2a indicates the gradient at the end of the column, which extends from 3 to 23 min. The 3-min delay of the gradient start in Fig. 2a corresponds to the equipment hold-up volume plus the column dead volume.

Peak capacity (PC) can be defined as the maximum number of bands that will fit within a chromatogram with a resolution of $R_s = 1.0$; see Fig. 2b, based on the separation of Fig. 2a (same conditions). For gradient elution, where peak width tends to be similar for each peak in the chromatogram and if peaks eluting before or after the gradient are not included,

$$\begin{aligned} \text{PC} &= (t_G/W) + 1 \\ &\approx t_G/W \text{ (for large values of PC)} \end{aligned} \quad (1)$$

(note that half of the first and last bands in Fig. 2b fall outside the gradient). Here, t_G is the gradient time, and W is the average baseline peak-width. In the example of Fig. 2b, $t_G = 20$ min and $W = 0.5$ min, so $\text{PC} = 40$. A maximum peak capacity (PC_{\max}) corresponds to a full-range gradient (0–100% B, or $0 < \varphi < 1$), as in Fig. 2b. For a partial gradient, where the gradient range is $\Delta\varphi$,

$$\text{PC} = \Delta\varphi \text{PC}_{\max} \quad (2)$$

2.1.1. Sample peak capacity PC^{**}

Sample peaks may not use the entire chromatogram space, as in the example of Fig. 2a where the first peak A elutes after the gradient starts (with a retention time $t_a = 7.5$ min), and the last peak B elutes before the end of the gradient (with a retention time $t_z = 15.5$ min). Peak capacity for a *given sample* and specified HPLC separation conditions (as in Fig. 2b) can be defined as “sample peak capacity”, PC^{**} , where

$$\text{PC}^{**} = (t_z - t_a)/W \quad (3)$$

The sample peak capacity for the example of Fig. 2a is illustrated in Fig. 2c, where $\text{PC}^{**} = 16$.

2.1.2. Required sample peak capacity PC^*

Assume that conditions (e.g., T and t_G) have been optimized for maximum sample resolution. The resulting resolution R_s for the critical (least resolved) band-pair $[(R_s)_{\max}]$ will in general not equal 1 for a given sample and other conditions, as in the example of Fig. 2a for which $(R_s)_{\max} = 1.6$. However, we wish to know the peak capacity PC^* that is *required* for this optimized separation, in order for $(R_s)_{\max} = 1$. The required sample peak capacity PC^* is of interest for reasons that will become clear in the following discussion.

We can use the observed sample peak capacity PC^{**} [with $(R_s)_{\max} \neq 1$] to obtain a normalized value PC^* [where $(R_s)_{\max} = 1$] as follows. If the value of R_s for the optimized separation is mathematically adjusted by a factor x (equivalent to a change in N such that bandwidth changes by $1/x$), the corresponding value of PC^{**} will change by the factor x (Eq. (2)). Therefore, the peak capacity PC^* required for $R_s = 1$ can be obtained from the observed peak capacity PC^{**} (where $R_s \neq 1$) as

$$\text{PC}^* = \text{PC}^{**}/(R_s)_{\max} \quad (4)$$

The example of Fig. 2d shows the chromatogram corresponding to this value of PC^* , equal to 10 in this case. In this example, $\text{PC}^* < \text{PC}^{**}$, because the required resolution ($R_s \geq 1$) is less than the actual resolution ($R_s = 1.6$). When $(R_s)_{\max} < 1$, then $\text{PC}^* > \text{PC}^{**}$, because the required resolution is then greater than the actual resolution.

2.1.3. Peak capacity PC as a function of experimental conditions

In gradient elution, we can increase peak capacity PC in either of two ways: (a) by using a longer gradient time t_G , or (b) by selecting conditions which increase the column plate number N . Either of these two options normally involves a longer run time. The combined effects of N and t_G on PC are summarized in Fig. 3 as a log–log plot of PC_{\max} vs. t_G , for otherwise optimized conditions and “typical” (small molecule) samples. The basis of Fig. 3 is given in the Appendix. For reasonable separation times (< 2 h), the maximum value of PC is no more than 250. If the gradient range $\Delta\varphi$ is adjusted so that the first

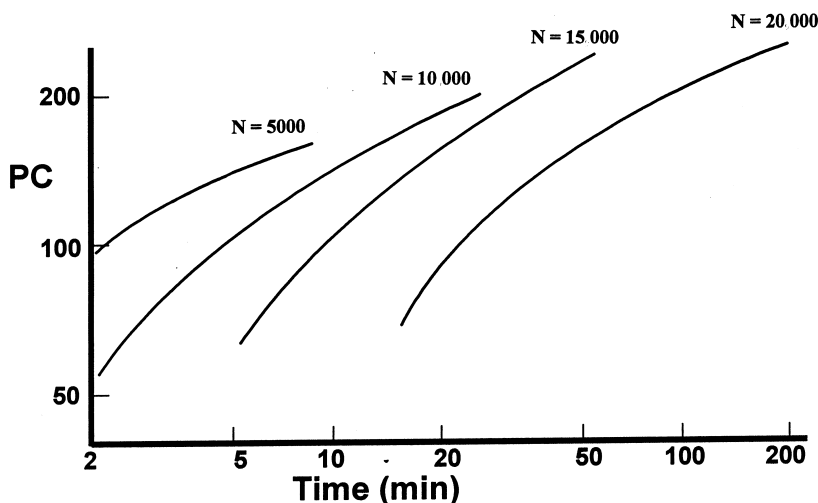


Fig. 3. Maximum peak capacity PC as a function of gradient time t_G for different column plate numbers (assumes $R_s = 1$). See the Appendix for details.

peak elutes at the start of the gradient and the last peak elutes at the end of the gradient, then (Eq. (2))

$$PC_{\max} \leq 250\Delta\varphi \quad (5)$$

Larger values of PC are in principle possible by the use of capillary electrochromatography (CEC), where values of N can exceed 100 000. However, unless noted otherwise, we assume conventional HPLC separation in the following discussion.

2.1.4. Peak capacity in isocratic vs. gradient elution

Similar definitions of peak capacity as in Fig. 2 apply for both isocratic and gradient elution. It has been shown elsewhere [11] that the resolution of two adjacent bands in both isocratic and gradient elution is identical, when values of % B (isocratic) and t_G (gradient) are adjusted to give the same retention factors (other conditions the same); i.e., similar values of k (isocratic) and k^* (gradient). Thus, an isocratic separation of the sample of Fig. 2 should result in similar incremental peak capacity values for each band-pair in the chromatogram, as for the corresponding gradient separation. Summing up these identical increments in each case will then result in identical peak capacities for each separation. While gradient elution results in band compression

[11], which might be thought to provide larger peak capacity values, this is largely compensated by a similar compression of the differences in retention times.

2.2. Resolution and selectivity

2.2.1. Isocratic optimization of the mobile phase

Given a sample peak capacity $PC^{**}=n$ for a sample that contains n components, it is not expected that all peaks within the chromatogram will be resolved with $R_s=1$. Probability considerations instead predict a random positioning of peaks, so that the resolution (with $R_s \geq 1$) of all peaks in a given sample containing n components will require $PC^* > n$ [2]. Fig. 1 provides a practical example of this conclusion, where $PC^{**}=168$ (much in excess of $n=48$), yet only 25 peaks are separated with $R_s \geq 1.0$. This point is illustrated further in Fig. 4 for isocratic separation, which is adapted from the study of Herman et al. [10]. Because isocratic and gradient separations are equivalent under “comparable” conditions of retention [11], it can be argued that the relationships of Fig. 4 should be similarly applicable for gradient elution. The lower curve (“ideal”) of Fig. 4 corresponds to a required peak capacity $PC^*=n$; this is the minimum value of PC^* that will allow the separation of all n peaks with $R_s \geq 1$; i.e., “ideal”

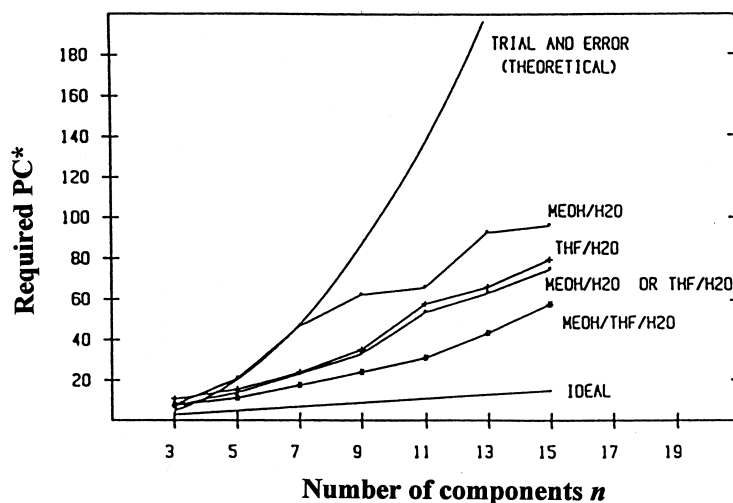


Fig. 4. Dependence of required peak capacity PC^* on number n of sample components for the separation of all bands with $R_s > 1$. See text for further details. Adapted from Ref. [10].

band spacing as in Fig. 2b–d. The upper curve in Fig. 4 (“trial and error”) assumes a random distribution of peak retention times (i.e., prior to attempts at optimizing selectivity) and is calculated from a well-established theory of separation vs. peak capacity [2]. This latter curve predicts the average value of PC^* for samples containing n components, with $R_s \geq 1$ for every peak-pair. For example, the required (“trial and error”) peak capacity for $n = 10$ is $PC^* \approx 115$.

Assuming that method development for a sample with $n = 10$ begins with a gradient run [1], and further assuming that $PC^{**} = 115$, there is predicted [2] to be a 50% chance that all peaks will be separated with $R_s \geq 1$ in this initial gradient run (this assumes that the “trial-and-error” curve of Fig. 4 also applies for gradient elution). However, further experiments chosen to change selectivity α are likely to result in a better peak spacing and improved separation (for optimized selectivity); this in turn means that a smaller peak capacity PC^* will in most cases be able to achieve $R_s \geq 1$ for all bands.

Representative experimental data have been used [10] to estimate the effect of such changes in selectivity on the required peak capacity PC^* for isocratic elution. For example, if methanol–water mobile phases are used, and % methanol (% MeOH)

is allowed to vary, an improvement in band spacing can be expected for some value of % MeOH. The required peak capacity PC^* for this optimum value of % MeOH is given by the plot in Fig. 4 labeled “MeOH/H₂O”. For $n = 10$, the value of PC^* is now only 65 (about half the “trial and error” value). This confirms what chromatographers already know: a systematic variation in selectivity will generally lead to a better peak spacing, an improved separation, and a decrease in the plate number or peak capacity that is required for $R_s \geq 1$.

Other plots of PC^* vs. n are shown in Fig. 4 for varying % tetrahydrofuran (“THF/H₂O”), varying % MeOH or % THF (“MeOH/H₂O” or “THF/H₂O”), or varying % MeOH and % THF in the ternary-solvent mobile phase MeOH/THF/H₂O (“MeOH/THF/H₂O”). As expected, when the number of possible changes in the mobile phase is increased (MeOH/H₂O = THF/H₂O < [MeOH/H₂O or THF/H₂O] < MeOH/THF/H₂O), a better selectivity can be achieved, and the value of PC^* required for separation with $R_s \geq 1$ decreases. By simultaneously varying THF, MeOH and water in the ternary-solvent mobile phase, the required value of PC^* for $n = 10$ is reduced to about 30 (i.e., $\approx 1/4$ the “trial and error” value of 115). Each of the various experimental curves of Fig. 4 represents an average

for many samples; for a given value of n , the value of PC* for a *specific* sample studied in [10] was observed to vary by about $\pm 30\%$ (1 SD).

The simultaneous variation of % MeOH and % THF in a MeOH–THF–water mobile phase corresponds to a change in two variables (once the MeOH and THF concentrations are chosen, the % water value is determined). Simultaneous changes in more than two experimental conditions have been reported [12–14]; however, the number of experiments required to optimize more than two variables can be quite large, so this approach is often impractical. Also, limited data [12–14] suggest that the incremental improvement in resolution via the simultaneous optimization of a third variable can be marginal.

2.2.2. Use of other variables for optimizing selectivity

The ability of different variables to control reversed-phase selectivity has been discussed [15]. It appears that average changes in α (as some experimental condition is varied) become larger in the sequence (ACN=acetonitrile): temperature (least effective) < mobile phase % organic \approx column type (e.g., C₁₈, cyano, phenyl) < mobile phase solvent type (MeOH/ACN < MeOH/THF \approx ACN/THF).

Here, MeOH/ACN, etc., refers to a change in B solvent (e.g., MeOH replaces ACN) as a means of optimizing selectivity. A change in gradient time t_G is equivalent to a change in isocratic % organic, so far as its effect on selectivity [11]. We can use the latter ranking of variables for a change in selectivity (and resolution) to compare method development approaches based on (a) simultaneously varying temperature and gradient time (equivalent to isocratic % B) vs. (b) the use of mobile phases where % MeOH and % THF are simultaneously varied (“MeOH/THF/H₂O” in Fig. 4). The latter approach corresponds to the simultaneous variation of MeOH/THF proportions *and* % B = (% MeOH + % THF). Because temperature is a less effective variable for controlling selectivity than is the variation of MeOH/THF, we might expect that approach *b* (MeOH/THF/H₂O) will be generally more effective than *a* (T , t_G). This hypothesis is examined further in the present study.

3. Experimental

Experimental data used in this study are described below or were reported previously [8,14,16–19]. These data have been used here with computer simulation (DryLab/for Windows Version 2.0, LC Resources, Walnut Creek, CA, USA) to determine values of PC* (after optimizing temperature and gradient time) for 24 different samples where $8 \leq n \leq 48$.

3.1. Calculations

The DryLab software provides two-dimensional resolution maps as a function of temperature and gradient time for a given sample [8], from which values of T and t_G can be determined that provide maximum sample resolution $(R_s)_{\max}$. Fig. 5 illustrates (previously unreported) resolution maps for four of the samples of Table 2; in each case, the cursor marks conditions for $(R_s)_{\max}$. Values of PC** were determined from computer-predicted values of retention time and average bandwidth for these optimized values of T and t_G (Eq. (3)). Finally, resulting values of $(R_s)_{\max}$ were used to calculate values of the adjusted peak capacity for $R_s = 1$ (equal to PC*) via Eq. (4). As an example of this calculation, consider the substituted benzoic acids sample of Table 2 (No. 1, pH 2.6). When temperature and gradient time were optimized (75°C, 29 min), the resulting (critical) resolution was $R_s = 1.66$. For these same conditions, the sample peak capacity PC** was equal to 37 (Eq. (2)). The required peak capacity PC* for a sample resolution of $R_s = 1$ is then $37/1.66 = 22$ (Eq. (4)). For those samples where peaks elute before or after the gradient, only peaks eluting within the gradient were considered. For example, the first two peaks of the benzoic acids sample eluted before the gradient in the separations where pH was equal to 3.7 and 4.3, so only the latter six peaks were considered for these separations.

3.2. New samples and conditions

Most of the samples of Table 2 and their separation have been reported previously (see Refs. in Table 2). Data for samples 15, 17, 20, 23 were obtained in this study.

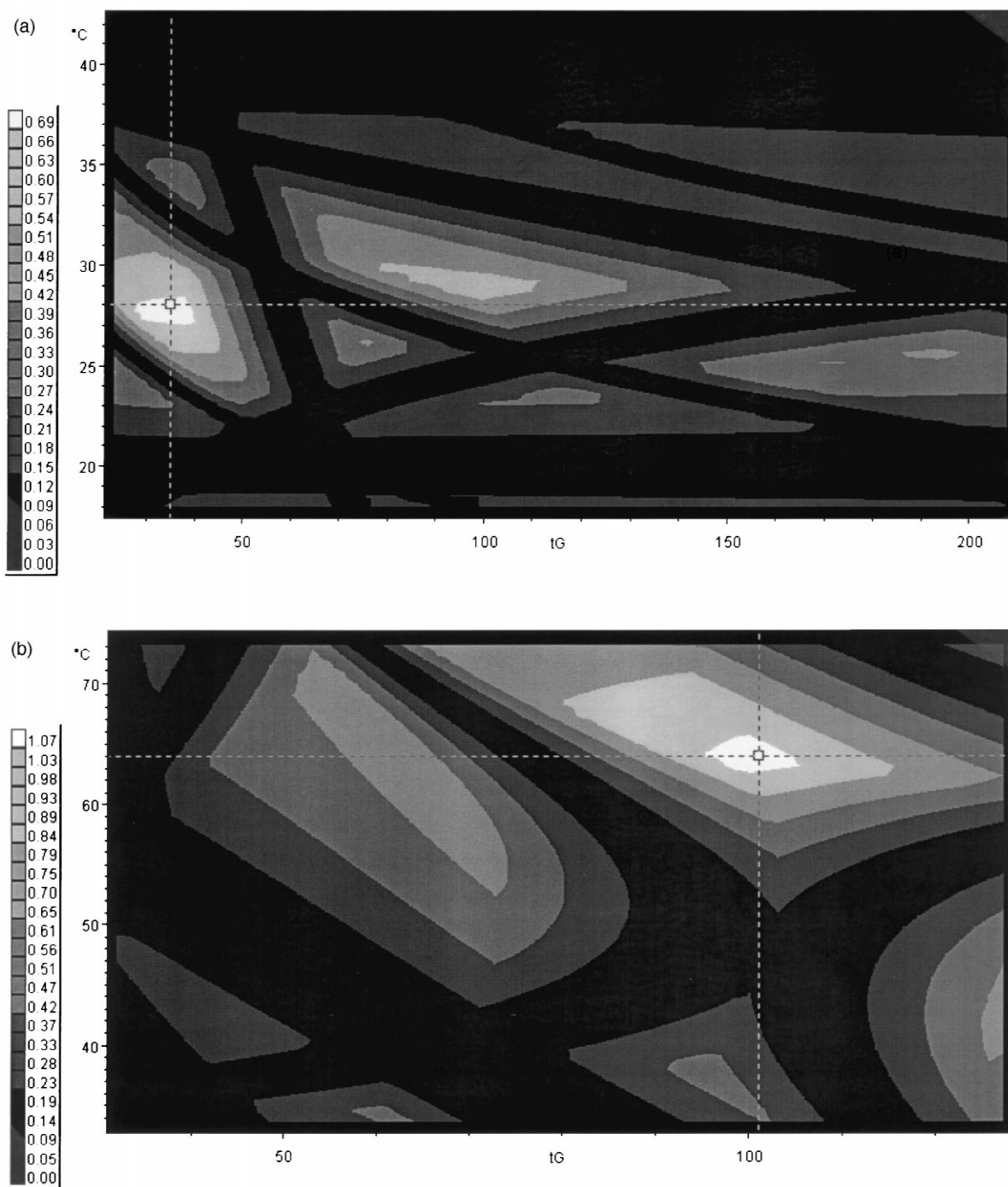


Fig. 5. Resolution maps for reversed-phase HPLC separation as a function of temperature ($^{\circ}\text{C}$) and gradient time t_G (min). (a) Separation of 19 herbicides at pH 3.5 (sample 15 of Table 2); (b) separation of 22 synthetic organics with methanol as B solvent and column 1 (sample 17 of Table 2); (c) separation of 33 synthetic organics (sample 20 of Table 2); (d) separation of 47 toxicology standards with acetonitrile as B solvent (sample 23 of Table 2). Resolution increases for lighter regions of each map, and in each case the cursor marks conditions for maximum resolution.

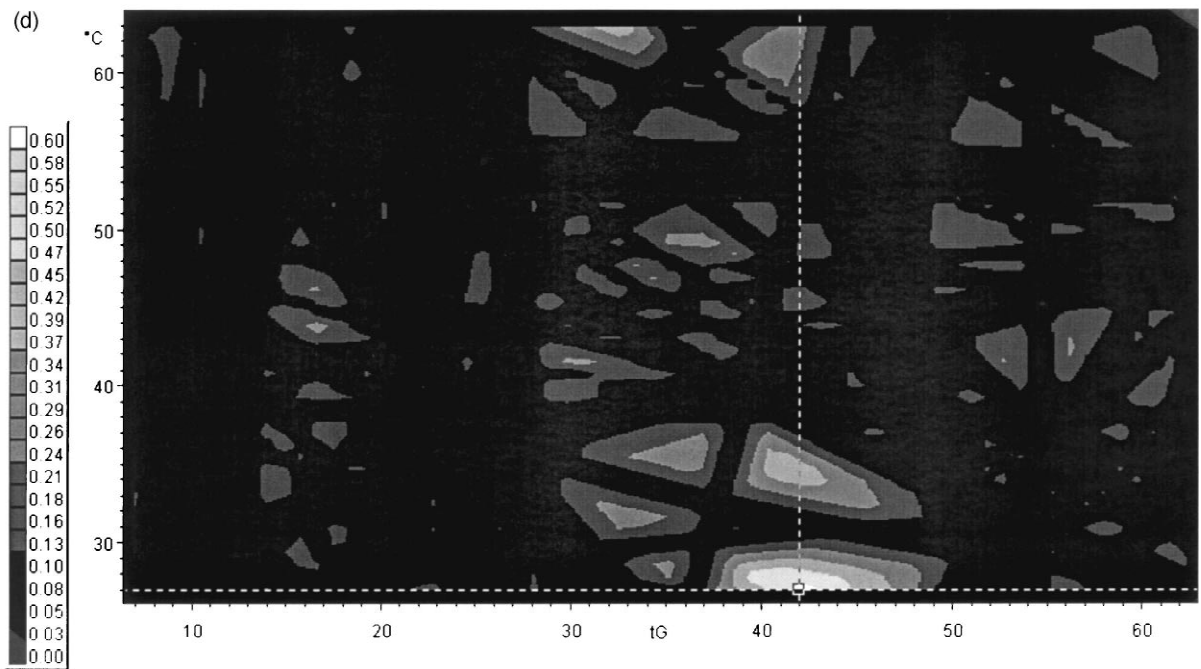
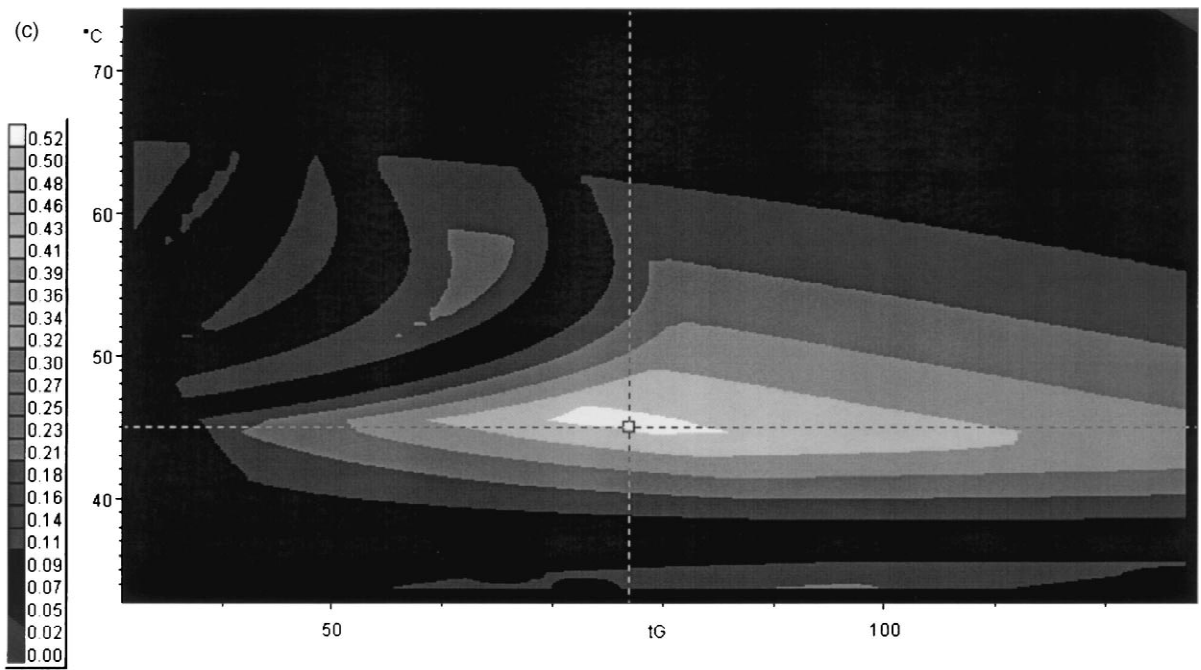


Fig. 5. (continued)

Table 2

Required peak capacity values PC* for samples of present study; assumes temperature and gradient time are optimized for maximum resolution.

Sample	Note ^a	Ref.	Optimum conditions ^b	PC** ^c	R _s ^d	PC* ^e	n ^f	Δφ ⁿ	
1	Substituted benzoic acids	[8,14]	pH 2.6	29 min, 75°C	37	1.66	22	8	0.15
			pH 3.2	13 min, 66°C	40	1.59	26	8	0.08
			pH 3.7	77 min, 31°C	30	2.17	14	6 ^g	0.06
			pH 4.3	77 min, 36°C	20	2.16	20	6 ^g	0.07
2	Substituted anilines	[8,14]	pH 2.6	12 min, 75°C	41	6.36	8	5 ^g	0.29
			pH 3.6	42 min, 31°C	85	2.32	37	9	0.40
			pH 4.6	27 min, 79°C	49	1.55	33	9	0.31
			pH 5.6	12 min, 74°C	39	1.72	24	9	0.31
3	Herbicide impurities	[8]	33 min, 38°C	99	4.91	21	9	0.33	
4	Pharmaceuticals	[8]	89 min, 49°C	147	5.91	26	9	0.50	
5	Corticosteroids	[8]	54 min, 27°C	39	1.07	37	9	0.14	
6	Synthetic organics	[8]	47 min, 42°C	93	2.58	37	11	0.44	
7	Algal pigments	[14]	Col-A ^h	68 min, 47°C	125	3.27	38	12	–°
Col-B ^h			20 min, 39°C	100	1.32	76	12	–°	
8	Herbicides	[8]	89 min, 34°C	78	1.57	50	13	0.20	
9	LSD derivatives	[8]	21 min, 59°C	38	0.77	50	13	0.31	
10	Fatty acid esters ^p	[14]	ACN ⁱ , col-B ^h	19 min, 62°C	45	0.32	139 ^p	13	0.25
			MeOH ⁱ , col-B ^h	154 min, 28°C	68	0.61	112 ^p	14	0.12
			ACN ⁱ , col-A ^h	84 min, 38°C	86	0.93	99 ^p	14	0.27
11	Acrylate monomers ^p	[8]	ACN ⁱ	30 min, 22°C	282	1.38	205*	14	0.89
			MeOH ⁱ	57 min, 34°C	331	1.31	253 ^p	14	0.88
12	Benzoic acids + anilines ^j	[17]	pH 2.6	27 min, 66°C	63	1.29	50	14	0.40
13	Basic drugs ^k	[16]		75 min, 52°C	122	1.95	63	15	0.33
14	Testosterones ^p	[8]		30 min, 42°C	59	0.20	289 ^p	17	0.21
15	Herbicides	– ^m	pH 2.7	56 min, 25°C	74	0.64	117	19	0.21
			pH 3.5	35 min, 28°C	54	0.69	80	19	0.20
16	Recombinant human growth hormone digest	[18]		203 min, 62°C	255	2.97	87	20	0.36
17	Synthetic organics	– ^m	Column 1, ACN	37 min, 68°C	91	0.54	170	21	0.30
			Column 2, ACN	37 min, 63°C	122	0.73	168	21	0.30
			Column 1, MeOH	101 min, 64°C	137	1.09	126	22	0.31
18	Nonbasic drugs ^k	[16]		45 min, 28°C	132	1.14	116	25	0.60
19	Algal pigments	[8]		80 min, 57°C	115	0.71	162	29	–°

Table 2 (continued)

Sample	Note ^a	Ref.	Optimum conditions ^b	PC** ^c	R_s ^d	PC* ^e	n^f	$\Delta\varphi^n$	
20	Synthetic organics	– ^m	77 min, 45°C	114	0.53	215	33	0.30	
21	rtPA protein triptic digest	[19]	91 min, 57°C	222	0.48	461	37	0.34	
22	Basic + nonbasic drugs ^l	[16]	31 min, 40°C	142	0.65	219	40	0.66	
23	Drug sample	ACN	– ^m	42 min, 27°C	172	0.61	283	47	0.44
		MeOH	– ^m	35 min, 44°C	144	0.43	334	47	0.54
24	No. 21 + nitroalkane standards ^l	[16]	64 min, 47°C	183	0.43	423	48	0.72	

^a Separation conditions (column, mobile phase organic solvent) noted when these (and only these) have been changed for a particular sample.

^b Conditions of temperature and gradient time that yield maximum sample resolution.

^c Sample peak capacity of the separation (Eq. (3)).

^d Maximum resolution, corresponding to specified conditions of temperature and gradient time.

^e Required peak capacity (Eq. (4)).

^f Number of sample components.

^g One or more sample components disregarded, when those components elute early or late in the gradient, thereby precluding accurate computer simulation for those peaks.

^h Col-A refers to a polymeric alkyl-silane column packing, col-B refers to a monomeric packing.

ⁱ ACN refers to acetonitrile as mobile phase solvent, MeOH to methanol.

^j Samples 1 and 2 were combined for this sample.

^k The basic drugs of Ref. [16] exclude early bands 1–7 of that study; sample 21 is a mixture of samples 22 and 13 of this table; sample 24 is a mixture of samples 13 and 18 plus eight internal standards from Ref. [16].

^m Samples from present study.

ⁿ Range in φ for sample peaks; see discussion of Fig. 7.

^o B solvents other than ACN or MeOH.

^p Samples excluded from Fig. 9.

3.2.1. Herbicides (No. 15 of Table 2)

This sample is an extension of sample 8. Additional commercial herbicides of similar molecular structure were added, but all other procedures, equipment and materials were unchanged. Conditions for input runs: 25×0.46 cm C₁₈ column; 5–70% B gradients in times of 40 and 120 min; A solvent is phosphate buffer, B solvent is acetonitrile; 1.5 ml/min; 20 and 35°C for pH 2.7 runs; 20 and 40°C for pH 3.5 runs. The dwell volume was 1.1 ml.

3.2.2. Synthetic organics (Nos. 17 and 20 of Table 2)

These were proprietary pharmaceutical discovery compounds of similar molecular structure (as in a combinatorial library), having an average molecular mass of about 600 and differing mainly in functional substitution. Procedures, equipment and materials were generally similar to those used for samples 6 and 9. Conditions for input runs: column 1 was a

25×0.2 cm YMC C₁₈; column 2 was a 25×0.3 cm Nucleosil C₁₈; gradients were variously 30–95% B or 40–100% B. The A solvent was water and the B solvent was either acetonitrile or methanol; flow-rates were 0.3 or 0.5 ml/min; temperatures were either 30 and 60°C or 37 and 70°C. The dwell volume was 1.2 ml. For the four runs used to optimize resolution in each of four computer simulation studies, only gradient time and temperature were varied.

3.2.3. Drug sample (No. 23 of Table 2)

Materials, equipment and procedures were similar as for sample 24, but the sample was almost entirely different. It consisted of the following 45 compounds plus two unidentified impurities: albuterol, 4-aminoantipyrine, ranitidine, norcodeine, ephedrine, nalorphine, cinchonidine, propionylprocainamide, nadolol, hydrocodone, pyrilamine, benzoylecgonine, antipyrine, brompheniramine, levorphanol, metoprolol,

naphazoline, zoxazolamine, thebaine, cocaine, phenacetin, doxapram, mazindol, colchicine, nefopam, fencamfamine, nitrazepam, mesoridazine, diphenhydramine, oxazepam, diazepam, flunixin, dibucaine, imipramine, cyclobenzaprine, tri-benzylamine, benzotropine, methadone, flunitrazepam, rescinnamine, “niflumic acid”, prazepam, halazepam, tamoxifen, danazol. Input runs were carried out with gradient times of 12 and 36 min, at 30 and 60°C. The dwell volume was 0.6 ml.

4. Results and discussion

4.1. Required peak capacity PC^* as a function of the number of sample components n (temperature and gradient time optimized)

Values of PC^* from Table 2 are plotted in Fig. 6

vs. n . A subjective solid curve has been drawn through these data points; the latter defines the approximate peak capacity PC^* that will be required to separate an average sample containing n components. Three different samples (noted by the larger squares, triangles and hexagon) have been excluded in the process of constructing this average curve for PC^* vs. n . The reason for omitting these data is that peak capacity depends upon sample molecular structure, as discussed next.

4.1.1. Peak capacity vs. sample molecular structure

When two or more compounds within a given sample are very similar in molecular structure (e.g., isomers), there is a greater probability that they will have a similar retention, resulting in a larger value of PC^* . Likewise, when a sample is composed predominantly of molecules which do not differ in terms

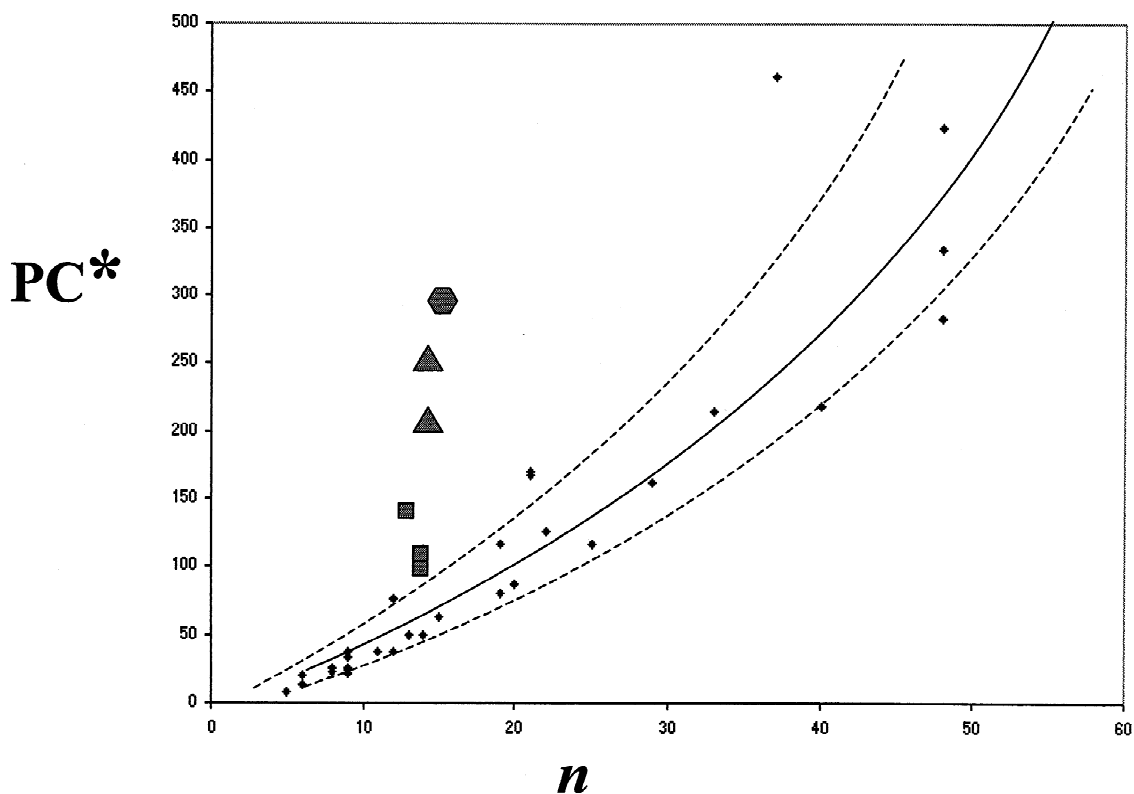


Fig. 6. Plot of required peak capacity PC^* vs. number of sample components n for samples where temperature and gradient time have been optimized. Data of Table 2; samples 10 (squares), 11 (triangles) and 14 (hexagon). Dashed curves are ± 1 SD, omitting samples 10, 11 and 14 (see text).

of polar substitution, it has been observed [15] that changes in T or t_G will have little effect on separation selectivity. This is equivalent to PC^* vs. n being described by the “trial-and-error” curve of Fig. 4. That is, samples in which there is limited substitution by the same polar functional group are expected to have larger values of PC^* for a given value of n . Among the samples of Table 2 (data for which are plotted in Fig. 6), three samples fit one of the foregoing descriptions and also stand out as obvious outliers in the plot of Fig. 6. Sample 10 (squares) consists of fatty acids that vary mainly in carbon number and olefinic unsaturation, but exhibit minimal differences in polar substitution. Sample 11 (triangles) has compounds differing mainly in carbon number, unsaturation and the presence of either one or two ester groups in the molecule. Sample 14 (hexagon) is composed of 14 hydroxytestosterone isomers plus three related compounds. The remaining samples of Table 2 and Fig. 6 are generally more diverse in terms of polar substitution (different polar groups and differing numbers of polar substituents). We believe that these remaining samples are also more representative of typical samples that require HPLC separation. Our following analysis therefore assumes that we are dealing with samples similar to those of Table 2, with the exception of samples 10, 11 and 14.

Because of the limited number of samples represented in Fig. 6, it is difficult to define uncertainty limits for the average (solid) curve through these data. The study of [10] is based on a much larger sample set for $3 \leq n \leq 15$, and from this study we can estimate the standard error in PC^* for each value of n . Assuming that this variation arises from random variations in sample structure, it is not unreasonable to assume a similar uncertainty for the data of Fig. 6. The dashed curves of Fig. 6 correspond to ± 1 SD derived in this way; i.e., from the data of Ref. [10]. These uncertainty limits appear not unreasonable, in terms of the observed distribution of data points in Fig. 6; in any case, they represent our present best estimate.

The maximum possible peak capacity PC_{\max} is given by Eq. (5), but this requires a determination of $\Delta\varphi$ (adjusted value for sample retention range) as a function of n . Values of $\Delta\varphi$ for the samples of Table 2 are plotted vs. n in Fig. 7; here, it is assumed that the first peak elutes at the start of the gradient, and

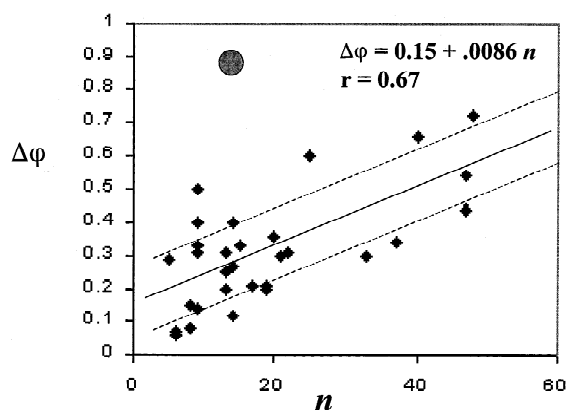


Fig. 7. Dependence of required retention range in gradient elution ($\Delta\varphi$) on the number of sample components n for samples of Table 2. In this case, $\Delta\varphi$ is equal to φ at elution for the last peak minus φ at elution for the first peak. The dashed lines are ± 1 SD; the large circle overlaps two excluded data points (sample 11).

the elution of the last peak corresponds to the end of the gradient. As expected, values of $\Delta\varphi$ tend to be larger as n increases, although the correlation is rather modest [$r=0.67$, if two obvious outliers (large circle) at the top of the figure are omitted (deviation equals five-times standard deviation for remaining points)]. The dashed curves in Fig. 7 correspond to ± 1 SD from the solid curve.

We have used this correlation ($\Delta\varphi=0.15+0.0086n$) with Eq. (5) to estimate maximum PC as a function of n (solid curve of Fig. 8). Also plotted in Fig. 8 (dashed curve marked “required”) is the solid curve from Fig. 6. The intersection of these two plots at $n=17$ indicates the maximum value of n for which there is a 50% probability that a sample can be separated with $R_s \geq 1$, after optimizing temperature and gradient time. Uncertainty limits (± 1 SD) are also indicated in Fig. 8, suggesting a considerable uncertainty (arrow at bottom of Fig. 8) in this maximum value of $n=17$.

If the resolution requirements for the final separation are changed, then the maximum value of n as found in Fig. 8 will also change. Thus, if baseline separation is the goal ($R_s \geq 1.5$), values of PC^* in Fig. 6 will be increased by 1.5-fold, and the maximum value of n (for 50% chance of separation in a single run) is decreased to only 12 components. Similarly, if resolution need be only large enough to recognize overlapping peaks ($R_s \leq 0.7$), the maximum value of n equals 21. Table 3 summarizes the

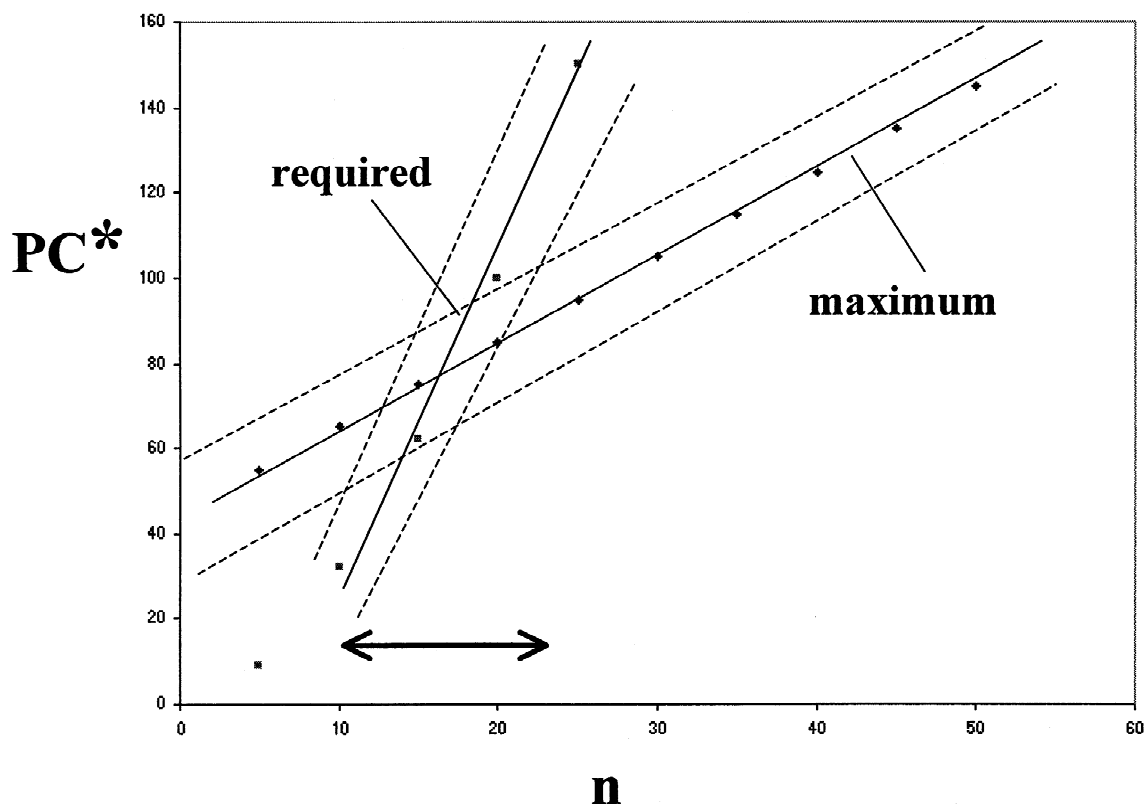


Fig. 8. Determination of the maximum number of sample components n that can be separated with $R_s \geq 1$ after optimizing temperature and gradient time. Solid curves indicate (a) maximum peak capacity PC^{**} as a function of n (Eq. (4)) and (b) the solid curve of Fig. 6. The dashed lines are ± 1 SD from each solid line. See text for details.

application of the preceding relationships to the separations of Table 2, by examining whether the required resolution was obtained for n less than or greater than the maximum value of n (n_{\max}). For $n < n_{\max}$, 81–86% of the separations have a resolution which exceeds that required. For $n \geq n_{\max}$, only 13–33% of the separations have a resolution that exceeds that required. These results can serve as

a rough guide of whether a given sample can be separated with some required resolution, when the number of sample components n is known. We conclude that the separation of samples with more than 15–20 components by a single HPLC run will often be challenging, when using temperature and gradient time to control selectivity and resolution.

Before leaving Figs. 6–8 and resulting implica-

Table 3

Separations of Table 2 that exceed the resolution requirement for different values of maximum n^a

Required value of R_s	Maximum n (n_{\max})	Success rate for $n < n_{\max}$	Success rate for $n \geq n_{\max}$
0.7	21	25/29 = 86%	3/9 = 33%
1.0	17	17/21 = 81%	5/17 = 29%
1.5	12	12/14 = 86%	3/24 = 13%

^a For example, for a required resolution $R_s = 1.0$, the maximum value of n is 17. There are 21 separations in Table 2 where $n < 17$, and 17 of these 21 separations have $R_s > 1.0$.

tions for separating complex samples, it is interesting to consider the impact of CEC with its higher possible plate numbers. If we assume that values of N can be four-fold greater than for corresponding HPLC separations (a reasonable guess), peak capacity values are doubled, and the maximum value of n is increased by about 50% (e.g., $n \leq 25$ for $R_s \geq 1$). This result can be obtained from Fig. 6, by superimposing the curve from Fig. 8 for “maximum PC”, after increasing all PC values by two-fold.

4.2. A comparison of different method development approaches based on required peak capacity PC^*

Recent papers [8,14,17] have reported data for several samples where simultaneous changes in temperature T and gradient time t_G were used to optimize selectivity and maximize resolution, as summarized in Table 2. However, no comparison of this approach with other two-variable optimization schemes (as in Table 1) has so far been attempted. Data from the study of Ref. [10] as summarized in Fig. 4 permit such a comparison: optimizing tem-

perature and gradient time (or isocratic % B) vs. the optimization of mobile phase composition (% MeOH and % THF varied). However, it must be emphasized that different samples were involved in these two studies, which therefore prevents any final conclusions. The samples of Fig. 4 consist of a large number of different combinations selected from 32 substituted benzenes. There is a substantial variation in the number and type of polar substituents for the components of these samples. With the exception of samples 10, 11 and 14, the samples of Table 2 (and Fig. 6) likewise exhibit significant differences in polar substitution, and for this reason there is no a priori reason to assume a sample bias in these two studies that would favor one approach or the other (T and t_G vs. % MeOH and % THF).

The data of Fig. 6 are re-plotted in Fig. 9 for the same range in n covered in Fig. 4. The dashed curves (calculated by us from the data of Ref. [10]) are for separations that have been optimized by varying the proportions of methanol, tetrahydrofuran and water in the mobile phase; these curves represent ± 1 SD uncertainty limits. With the exception of data for

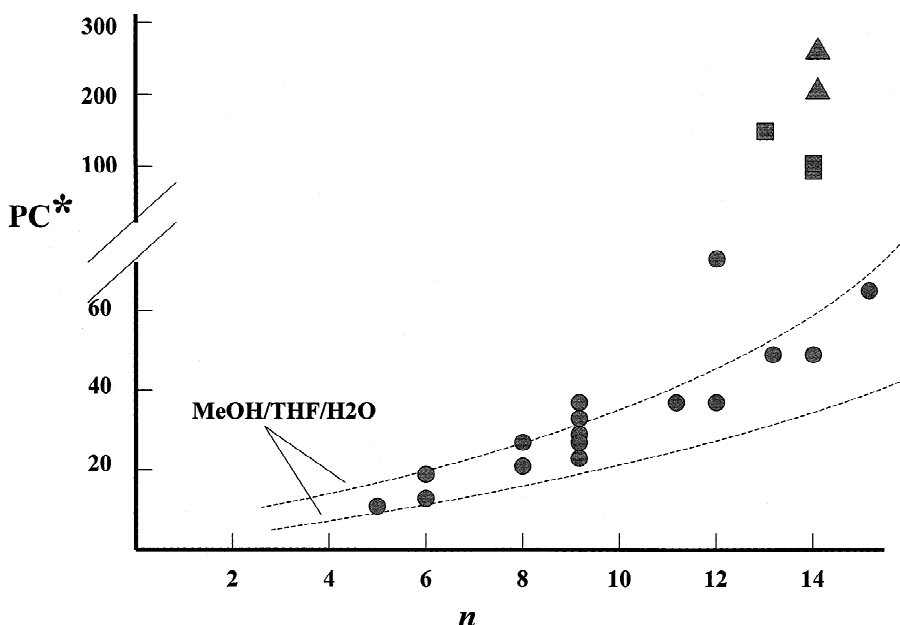


Fig. 9. Comparison of the effectiveness of temperature–gradient time optimization vs. optimization of mobile phase composition (methanol, THF, water mixtures) in maximizing sample resolution. Data points are for $T-t_G$ optimization (Table 2), with samples 10 (squares), 11 (triangles) and 14 (hexagon). The dashed curves are uncertainty limits (± 1 SD) for the MeOH/THF/H₂O curve of Fig. 4 (optimized % MeOH and % THF). See text for details.

samples 10 (squares); 11 (triangles), and 14 (hexagons), the data of Table 2 appear to overlap the data of Ref. [10], but with a *slight* apparent preference for optimizing % MeOH and % THF. There thus appears to be little difference in these two method development approaches (varying T and t_G vs. varying ACN, MeOH and water) in their ability to optimize selectivity and maximize resolution. That is, the limiting value of n for samples that can be separated with $R_s \geq 1$ is about the same in each case.

Elsewhere (see discussion of Table 6 of Ref. [8]), we have noted that the maximum resolution that can be attained by varying T and t_G usually increases as the range in T and t_G increases (a corresponding argument cannot be used to increase R_s for the separations of Fig. 4). The average change in T and t_G that was explored in the examples of Table 2 is considerably less than “practical” limits of 60°C and a factor of 5- to 10-fold in t_G . If this “sub-optimal” application of T - t_G optimization in Table 2 is taken into account, as well as uncertainty in the “comparability” of samples used in the two studies, the two plots of Fig. 9 become indistinguishable within experimental error. *However, it must be recognized that any comparison of selectivity control that is not based on the same samples is highly tentative.* Only when a large number of diverse samples are compared as in Fig. 9 (with the *same* samples used for both solvent type and T - t_G optimization) will any final conclusion be possible.

The comparison of Fig. 9 is independent of separation time, but peak capacity does vary with the allowed run time (Fig. 3). Also, gradient elution is more efficient than isocratic separation in terms of peak capacity. However, these considerations do not affect our comparison of solvent type vs. T - t_G optimization in terms of their relative effectiveness for sample separation. In view of the (surprising) similarity of plots of PC* vs. n for the two selectivity-optimization approaches compared above and in Fig. 9, we suggest that other two-variable method development procedures as in Table 1 *may* be similarly effective in maximizing sample resolution (see discussion of [15]). However, because different samples will respond differently to a change in different variables, such a hypothesis will be very difficult to prove for the general case.

5. Conclusions

The present investigation has applied the concept of “required sample peak capacity” PC* to address two questions which relate to method development based on the simultaneous optimization of temperature T and gradient time t_G : (1) what maximum number of components n can a sample contain, with a reasonable likelihood for the total separation of the sample in a single reversed-phase HPLC run? (2) How does the simultaneous adjustment of T and t_G compare with changes in solvent type (% MeOH and % THF) for the optimization of selectivity and the maximization of sample resolution?

It appears that typical samples can contain 15 to 20 components, with at least a 50% probability that a resolution of $R_s \geq 1$ can be achieved by optimizing T and t_G . If baseline resolution ($R_s \geq 1.5$) is required, the maximum number of compounds is 10 to 15. On the other hand, if only a recognizable peak resolution ($R_s \geq 0.7$) is needed, the maximum number increases to 20 to 25. These estimates of maximum n depend strongly on the nature of the sample and the range in values of T and t_G which are explored. Samples whose molecules show little variation in the number or type of polar substituents will be more difficult to separate. If a maximum range in T (e.g., 60°C) and t_G (e.g., by 5- to 10-fold) is explored, the maximum value of n is expected to increase somewhat.

The optimization of T and t_G was also compared with the variation of mobile phase composition (% MeOH and % THF). It appears to us that either of these two procedures can provide comparable sample resolution, and therefore both method development approaches are probably limited to a similar maximum values of n . This observation is surprising, since the ability of *either* T or t_G to vary band spacing and maximize separation is much less than has been observed for changes in solvent type (e.g., varying the ratio of MeOH to THF). We speculate that this *may* be generally true for the use of other separation variables in method development, when two or more variables are simultaneously optimized as in the present study. However, no direct evidence for this suggestion has yet been provided to our knowledge.

Changes during method development of tempera-

ture and either gradient time or isocratic % B are much more convenient than are changes in other variables and are more easily automated for unattended experiments. Methods developed by optimizing T and t_G also tend to be more reliable and robust [15–17]. For this reason, we recommend the optimization of T and t_G as an initial approach for HPLC method development.

6. Glossary of terms

Symbols defined here include those used in following papers [9,24].

$a, b, a', b', A, B, A', B', A'', B''$, Constants in various equations

b , Gradient steepness parameter

A, B, A- and B-solvents which are mixed to form the mobile phase

CEC, Capillary electrochromatography

C1, C2, C3, C4, C5, Abbreviations for various *o*-dialkylphthalates (see Experimental section of Part III)

$E_T(30)$, Solvatochromic mobile phase parameter

F , Flow-rate (ml/min)

i, j , Refers to adjacent bands i and j

k , Solute retention factor (isocratic)

k_1, k_2 , Values of k for different values of φ (input values)

k^* , Solute retention factor (gradient); $k^* = 0.85t_G F / (V_m \Delta\varphi S)$

k^*_1, k^*_2 , Values of k^* for different gradient times t_{G1} and t_{G2} (input values)

k_w , Extrapolated value of k for 0% B ($\varphi = 0$)

L , Column length (cm)

LSS, Linear-solvent-strength (model)

M_r , Molecular mass

n , Number of components in the sample

N , Column plate number

PC, Peak capacity; equal to the maximum number of peaks that will fit within a given chromatogram with $R_s \geq 1$ (see Fig. 2b of Part I)

PC*, Sample peak capacity required for a resolution $R_s = 1$ for the “critical” band-pair (see Fig. 2d of Part I)

PC**, Sample peak capacity (see Fig. 2c of Part I)

R_s , Resolution, equal to $\Delta t_R / W$

$(R_s)_{\max}$, Maximum value of the “critical” resolution for a given sample, after optimizing T and t_G

RSD, Relative standard deviation

S , Solute parameter defined by Eq. (1)

t_a, t_z , Retention times for first and last peaks in the chromatogram

t_D , Gradient “dwell” (hold-up) time (min)

t_G , Gradient time (min)

t_{G1}, t_{G2} , Gradient times 1 and 2

t_0 , Column dead time (min)

t_R , Retention time (min)

t_{sec} , Retention time for a non-retained solute that may be partially excluded from the pores of the packing

T , Temperature ($^{\circ}\text{C}$)

T_K , Temperature (K)

T_1, T_2 , Temperature T for band 1 or 2

V_m , Column dead volume (ml)

W , Baseline bandwidth (min)

α , Separation factor

φ , Volume fraction of B solvent in the mobile phase; $\varphi = 0.01$ (%B)

φ^* , Value of φ in gradient elution when a band has migrated to the column midpoint

$\delta k, \delta k^*$, An error in a predicted value of k or k^*

δt_R , Error in a predicted value of t_R (min)

$\delta\varphi$, Error in the predicted value of φ of a band at elution; related to errors in predicted retention time by Eq. (1) (isocratic) and Eq. (4) (gradient) (Part III)

$(\delta\varphi)_i, (\delta\varphi)_j$, Values of $\delta\varphi$ for adjacent bands i and j

$\delta\delta\varphi$, An error in predicted resolution due to errors in predicted retention; equal to $(\delta\varphi)_j - (\delta\varphi)_i$

$\delta\delta\varphi(a)$, An average interpolated value of $|\delta\delta\varphi|$

$\delta\delta\varphi(m)$, A maximum interpolated value of $|\delta\delta\varphi|$

$\Delta\log \alpha$, Average change in $\log \alpha$ as a result of a change in some separation conditions; a general measure of selectivity

$\Delta\varphi$, Change in φ during a gradient; also, the range in φ required to elute a particular sample (Eq. (5) and Fig. 7 of Part I)

ΔT , Difference in T for input runs used to optimize T ($^{\circ}\text{C}$)

Δt_R , Difference in t_R for two adjacent bands

Acknowledgements

The present study was supported in part by a Small Business Innovation Research (SBIR) grant from the National Institutes of Health (US Department of Health and Human Services).

Appendix

Maximum peak capacity PC_{max} as a function of experimental conditions

A.1. Effect of gradient time or steepness on PC

We will assume [20] that isocratic retention for reversed-phase HPLC is given as

$$\log k = \log k_w - S\varphi \quad (\text{A.1})$$

Here, k_w is the (extrapolated) value of k for water as mobile phase ($\varphi=0$), φ is the volume-fraction of organic in the mobile phase (% B/100), and S is a constant for a given solute when only φ is varied. If a linear gradient is used, and Eq. (A.1) holds, then the separation is referred to as *linear-solvent-strength* (LSS) gradient elution [11]. Band width under LSS conditions is given as

$$W = (4/2.3)N^{-1/2}Gt_0(2.3b + 1)/b \quad (\text{A.2})$$

where N is the column plate number, G is a band compression factor whose value decreases with increasing gradient steepness, t_0 is the column dead time, and b is a gradient steepness parameter defined as

$$b = V_m \Delta\varphi S / (t_G F) = t_0 \Delta\varphi / t_G \quad (\text{A.3})$$

Here, $\Delta\varphi$ is the change in φ during the gradient ($\Delta\varphi=1$ for a 0–100% B gradient). Combining Eqs. (2), (A.2) and (A.3) yields

$$PC = (2.3/4)N^{1/2} \Delta\varphi^2 S / G(2.3b + 1) \quad (\text{A.4})$$

Peak widths observed in practice roughly correspond to Eq. (A.2) with $G=1$. Eq. (A.4) can therefore be rewritten as

$$PC \approx (2.3/4)N^{1/2} \Delta\varphi^2 S / (2.3b + 1) \quad (\text{A.5})$$

PC in Eq. (A.5) is observed to depend on b , which in turn is a function of column dimensions (V_m) and flow-rate F . Column length, flow-rate and particle size can be selected for a given value of N in the shortest run time (following section), which then defines PC as a function of run time (as in Fig. 3).

A.2. Column plate number N and PC

The plate number N and run time can be affected by changes in flow-rate, column length and/or particle size [1]. However, simultaneous changes in these variables are restricted by the maximum allowable column pressure. Given a maximum column pressure (e.g., <2000 p.s.i.; 1 p.s.i.=6894.76 Pa), maximum values of N per unit time can be obtained by working close to this pressure. Fig. 10 illustrates how values of N depend on run time for different combinations of column length, flow-rate and particle size. The upper envelope of these plots (dotted line) represents the maximum plate number N as a function of run time. The data of Fig. 10 correspond to $k=5$ for isocratic separation, so that t_0 equals 1/6-times the run-time values of this figure. The dotted curve of Fig. 10 be expressed as

$$\text{maximum } N \approx 10^4 t_0^{1/4} \quad (\text{A.6})$$

where t_0 is in min. Corresponding values of N for gradient elution will be similar. Eq. (A.3) can be rewritten as

$$t_G = \Delta\varphi(S/b)t_0 \quad (\text{A.7})$$

For small molecules, $S \approx 4$ [21], and $\Delta\varphi$ is assumed equal to 1 (maximum value of PC), so that

$$t_G \approx 4t_0/b \quad (\text{A.8})$$

PC vs. run time can now be estimated as a function of the required plate number N and gradient steepness b , by means of Eqs. (A.5) and (A.6). These results are plotted in Fig. 3. Each of the curves of Fig. 3 corresponds to a practical range in b ($0.1 < b < 1$). A deliberate increase in N to increase peak capacity is usually of marginal value, since N varies as (run time)^{1/4} (Eq. (A.6)), and therefore (Eq. (A.5)) PC varies as (run time)^{1/8}, when only N is changed, pressure is held constant, and flow-rate, column length and particle size are optimized for maximum

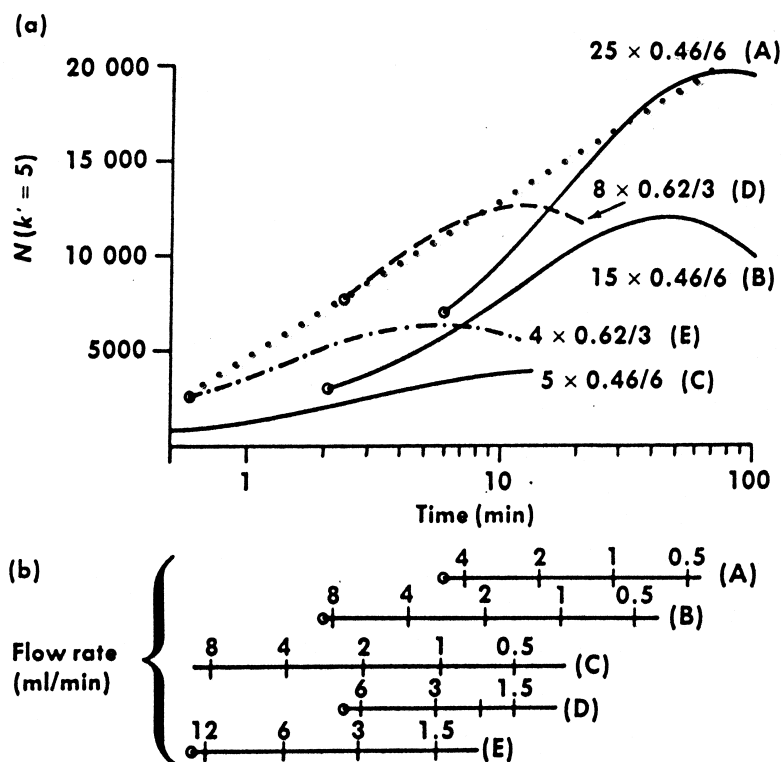


Fig. 10. Plate number of porous-particle columns as a function of column conditions. Representative conditions for small molecules as solute. Open circles represent maximum column pressure. The numbering for each curve (e.g., $25 \times 0.46/6$) refers to [column length, cm] \times [column diameter, cm]/[particle size, μm]. See Appendix 1 for details; adapted from Ref. [23].

N . Note also (Eq. 2) that a reduced gradient range $\Delta\varphi$ results in a shorter run time in Fig. 10.

For larger molecules, S increases with molecular mass M_r [22] as

$$S \approx 0.48M_r^{0.44} \quad (\text{A.9})$$

Eq. (A.9) has been shown to apply for peptide, proteins and polystyrene fractions, using acetonitrile as B solvent. According to Eq. (A.5), this should lead to larger PC values for larger molecules, but this effect is canceled to a large extent by a corresponding decrease in N for larger molecules.

References

- [1] L.R. Snyder, J.J. Kirkland, J.L. Glajch, Practical HPLC Method Development, 2nd ed., Wiley-Interscience, New York, 1997.
- [2] J.M. Davis, J.C. Giddings, Anal. Chem. 53 (1983) 418.
- [3] J.L. Glajch, J.J. Kirkland, K.M. Squire, J.M. Minor, J. Chromatogr. 199 (1980) 57.
- [4] J.W. Weyland, C.H.P. Bruins, D.A. Doornbos, J. Chromatogr. Sci. 22 (1984) 31.
- [5] R.C. Kong, B. Sachok, S.N. Deming, J. Chromatogr. 199 (1980) 307.
- [6] J.J. DeStefano, J.A. Lewis, L.R. Snyder, LC-GC Mag. 10 (1992) 130.
- [7] B. Bourguignon, P.F. de Agular, M.S. Khots, D.L. Massart, Anal. Chem. 66 (1994) 893.
- [8] J.W. Dolan, L.R. Snyder, N.M. Djordjevic, D.W. Hill, D.L. Saunders, L. Van Heukelem, T.J. Waeghe, J. Chromatogr. A 803 (1998) 1.
- [9] J.W. Dolan, L.R. Snyder, N.M. Djordjevic, D.W. Hill, T.J. Waeghe, J. Chromatogr. A 857 (1999) 21.
- [10] D.P. Herman, H.A.H. Billiet, L. DeGalan, Anal. Chem. 58 (1986) 2999.
- [11] L.R. Snyder, J.W. Dolan, Adv. Chromatogr. 38 (1998) 115.
- [12] J.S. Kiel, S.L. Morgan, R.K. Abramson, J. Chromatogr. 485 (1989) 585.
- [13] J.L. Glajch, J.C. Gluckman, J.G. Charikovskiy, J.M. Minor, J.J. Kirkland, J. Chromatogr. 318 (1985) 23.

- [14] J.W. Dolan, L.R. Snyder, D.L. Saunders, L. Van Heukelem, J. Chromatogr. A 803 (1998) 33.
- [15] L.R. Snyder, J. Chromatogr. B 689 (1997) 105.
- [16] P.L. Zhu, L.R. Snyder, J.W. Dolan, N.M. Djordjevic, D.W. Hill, L.C. Sander, T.J. Waeghe, J. Chromatogr. A 756 (1996) 21.
- [17] I. Molnar, L.R. Snyder, J.W. Dolan, LC·GC Int. 11 (1998) 374.
- [18] W. Hancock, R.C. Chloupek, J.J. Kirkland, L.R. Snyder, J. Chromatogr. A 686 (1994) 31.
- [19] R.C. Chloupek, W.S. Hancock, B.A. Marchylo, J.J. Kirkland, B. Boyes, L.R. Snyder, J. Chromatogr. A 686 (1994) 45.
- [20] K. Valkó, L.R. Snyder, J.L. Glajch, J. Chromatogr. A 656 (1993) 501.
- [21] L.R. Snyder, J.W. Dolan, J. Chromatogr. A 721 (1996) 1.
- [22] M.A. Stadalius, M.A. Quarry, T.H. Mourey, L.R. Snyder, J. Chromatogr. 358 (1986) 17.
- [23] L.R. Snyder, P.E. Antle, LC Mag. 3 (1985) 98.
- [24] J.W. Dolan, L.R. Snyder, R.G. Woplcott, P. Haber, T. Baczek, R. Kaliszan, J. Chromatogr. A 857 (1999) 41.